

RSC Advances



This is an *Accepted Manuscript*, which has been through the Royal Society of Chemistry peer review process and has been accepted for publication.

Accepted Manuscripts are published online shortly after acceptance, before technical editing, formatting and proof reading. Using this free service, authors can make their results available to the community, in citable form, before we publish the edited article. This *Accepted Manuscript* will be replaced by the edited, formatted and paginated article as soon as this is available.

You can find more information about *Accepted Manuscripts* in the [Information for Authors](#).

Please note that technical editing may introduce minor changes to the text and/or graphics, which may alter content. The journal's standard [Terms & Conditions](#) and the [Ethical guidelines](#) still apply. In no event shall the Royal Society of Chemistry be held responsible for any errors or omissions in this *Accepted Manuscript* or any consequences arising from the use of any information it contains.

1 **Facile and Green Cinchonidine-Assisted Synthesis of**
2 **Ultrafine and Well-Dispersed Palladium Nanoparticles**
3 **Supported on Activated Carbon with High Catalytic**
4 **Performance**

5 Tran Si Bui Trung,^a Yeonwoo Kim,^a Sehun Kim,^a Hangil Lee^{*b}

6 ^a*Molecular-Level Interface Research Center, Department of Chemistry, KAIST, 305-701, Republic of*
7 *Korea*

8 ^b*Department of Chemistry, Sookmyung Women's University, Seoul 140-742, Republic of Korea. Phone:*
9 *+82-2-710-9409. Fax: +82-2-2077-7321. E-mail: easyscan@sookmyung.ac.kr (H. Lee)*

10

11 **Abstract**

12 We report the facile and green synthesis of activated carbon-supported palladium (Pd/AC)
13 containing homogeneously dispersed Pd nanoparticles (Pd NPs) by using eco-friendly and
14 naturally available cinchonidine (CD) as the capping agent. The Pd NPs in the synthesized
15 Pd/AC hybrid are uniform with sizes predominantly in the range 4 to 7 nm. The synthesized
16 Pd/AC was characterized with various methods, such as TEM, XRD, and XPS, and the influence
17 of the synthetic conditions on its properties were investigated. The advantages of CD over
18 conventional capping agents include its easy depletion after the synthesis with a simple rinsing
19 process. Owing to the ultrafine, well-dispersed and purified Pd NPs, the synthesized hybrid
20 exhibits excellent catalytic activities in the reduction of 4-nitrophenol and methylene blue. These
21 findings further the development of novel stabilizing agents from naturally available sources for
22 the preparation of heterogeneous catalysts with enhanced performance.

23

24

25

26 1. Introduction

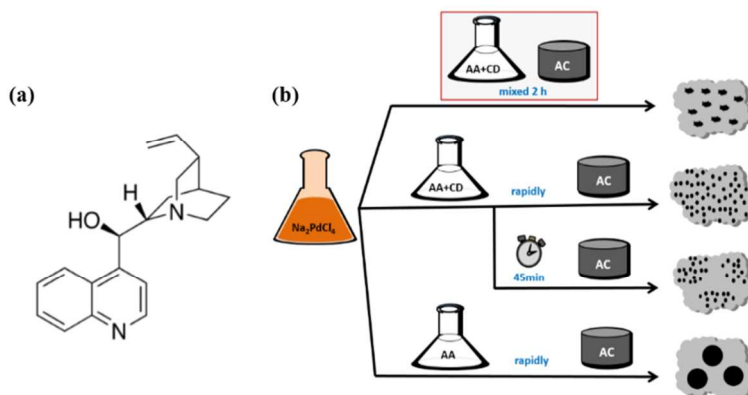
27 Palladium nanoparticles (Pd NPs) are among the most intensively used noble metals in
28 catalysis owing to their excellent catalytic performance in a variety of reactions.¹⁻³ Nonetheless,
29 there are difficulties inherent in the use of colloidal Pd NPs in homogeneous systems,
30 particularly in separation and subsequent recycling. Moreover, to meet the demand of high
31 performance catalytic applications, synthesized Pd NPs require a sufficiently small particle size
32 with a homogeneous distribution; however, these properties are impeded by inter-particle
33 aggregation due to the increase in the total surface energy as the size of Pd NPs decreases. One
34 of the most common and effective strategies to overcome these shortcomings is the solution-
35 phase deposition of Pd NPs onto a pre-existing nanostructured support.⁴⁻⁶ Although there have
36 been many attempts to improve the synthetic method, several problems still persist. Firstly, many
37 harmful chemical compounds, ranging from organic solvents (DMF, ethylene glycol, *etc.*) to
38 inorganic reagents (NaBH₄, hydrazine, *etc.*) are conventionally employed, which pose
39 environmental risks and threaten human safety. Next, the synthetic process generally requires
40 multi-step preparation under heat treatment, which results in high production costs and
41 asynchronous yields that limit commercial applications. Lastly, the presence of capping agents
42 severely limits the catalytic activities of the metal NPs. Therefore, the development of state-of-
43 the-art synthetic methods that can produce high performance supported Pd catalysts and address
44 the abovementioned disadvantages is highly desirable.

45 Pd NPs supported on carbon-based nanomaterials have been paid intensive attention due to
46 their potential applications in various fields.^{7,8} Many previously reported works related to
47 Pd/carbonaceous material based nanocatalysts have showed high efficiency in catalytic
48 performance. Z. Zhang *et al.* reported a unique Pd NPs loaded hierarchically porous graphene
49 network obtained by multiple synergistic interactions.⁹ The synthesized architecture showed
50 excellent activity and durability in ethanol oxidation due to the ultrafine monodispersed Pd NPs,
51 the strong interaction between Pd NPs and the support, and the unique hierarchically porous
52 network structure. Z. Wang *et al.* reported a highly efficient hydrogen generation from formic
53 acid/sodium formate aqueous solution catalyzed by *in situ* synthesized Pd/Carbon with citric
54 acid.¹⁰ The presence of citric acid during the formation and growth of the Pd NPs on carbon can

55 drastically enhance the catalytic property of the resulted Pd/Carbon. Among the most commonly
56 employed carbon materials as supports for metal-based catalysts in industrial applications is
57 activated carbon (AC) because it is cheap and it has a large surface area as well as high
58 resistance to acidic and basic media.¹¹

59 The recent tremendous advances in nanoscience and nanomaterials have led to robust
60 developments in chemical industries and manufacturing, but pose serious problems for the
61 preservation of the environment and the protection of human health. To establish sustainable
62 nanotechnologies, the design and usage of environmentally friendly chemicals and processes that
63 minimize the consumption as well as the generation of hazardous substances in every
64 technological area have been essentially emphasized.¹² Typically, a “green” synthesis of metal-
65 based catalysts involves the employment of products from natural or environmentally benign
66 sources, such as vitamins,¹³ tea and coffee,¹⁴ or sugars¹⁵ in nontoxic media under mild reaction
67 conditions. Hence, a particularly exciting challenge is to search for facile synthetic pathways and
68 novel eco-friendly chemicals that can achieve high catalytic efficiencies and satisfy the
69 principles of *Green Chemistry*.¹⁶ Ascorbic acid (AA), commonly known as vitamin C, is among
70 the most extensively used reducing agents for this purpose because it is biodegradable,
71 environmentally benign, naturally available, and has low toxicity.^{17,18} Cinchonidine (CD) is one
72 of the main components of the bark extracted from the plants belonging to the Cinchona species,
73 and is well-known as a catalyst for asymmetric organocatalysis, a ligand for transition metal
74 complexes, and a surface modifier for asymmetric heterogeneous reactions.¹⁹⁻²¹ Like other
75 cinchona alkaloids, CD is a relatively small molecule (M=294g/mol) comprising an aromatic
76 quinoline and an aliphatic quinuclidine moieties that are connected by two C–C bonds to form
77 different stereometric conformations.^{22,23} CD is a promising material from the view of *Green*
78 *Chemistry* because this organic chemical is naturally occurring, eco-friendly, biodegradable, and
79 nontoxic. To date, there have been only a few reports of colloidal metal syntheses using
80 derivatives of CD as stabilizers with modest catalytic performances.^{24,25} Furthermore, there have
81 been no reported studies for the applications of CD as a capping agent in the synthesis of
82 supported metal catalysts.

83 In the present paper, we come forward some significant advances in the synthesis of
84 supported Pd catalysts. First, we introduce a facile one-pot approach to the fabrication of an
85 activated carbon-supported palladium (Pd/AC) hybrid with ultrafine and homogeneously
86 dispersed Pd NPs. This synthesis is genuinely green since it utilizes CD as an efficient capping
87 agent for the first time and AA as a mild reductant in an aqueous medium at room temperature.
88 Next, we demonstrate that the removal of residual CD after catalyst preparation can easily be
89 achieved with a simple rinsing step, in contrast to the inherent problems of using conventional
90 capping agents; thus, making the present approach to catalytic applications more profitable.
91 Owing to the ultrafine, well-dispersed, and purified Pd NPs, the prepared Pd/AC catalyst exhibits
92 excellent catalytic performances in the borohydride reductions of 4-nitrophenol and methylene
93 blue (MB) under mild aqueous conditions.



94
95 **Fig. 1** (a) The cinchonidine (CD) molecule and (b) a schematic diagram of the method for the preparation
96 of the Pd/AC hybrids.

97 2. Experimental section

98 2.1 Chemicals

99 All reagents were of analytical grade and used as received without further purification. AC
100 (Darco, powder, -100 mesh), AA (99%), CD (96%), Na₂PdCl₄ (99.99%), NaBH₄ (powder,
101 ≥98%), 4-nitrophenol (powder, spectrophotometric grade), and MB (powder, dye content ≥82%)
102 were purchased from Sigma-Aldrich. Double distilled water was used in catalyst preparation, in
103 reduction reactions, and in all of the rinse processes.

104 2.2 Preparation of Pd/AC samples

105 The AC suspension was prepared by ultrasonicated 100 mg AC in 15 mL H₂O for 30
106 minutes followed by 1 hour of stirring. The Na₂PdCl₄ solution was prepared by ultrasonicated
107 14 mg Na₂PdCl₄ in 5 mL H₂O for 10 minutes. All the synthetic processes were carried out under
108 vigorous stirring (1000 rpm).

109 The Pd/AC(wash) hybrid was synthesized as follows. A mixture containing 30 mg AA and
110 20 mg CD in 15 mL H₂O was thoroughly ultrasonicated for 20 minutes to complete the
111 dissolution of AA and CD. The Na₂PdCl₄ solution was then added, and the resulting mixture was
112 rapidly added to the AC suspension. The suspension was stirred for 3 hours and then filtered,
113 washed (see the section 'Rinsing process'), and dried in the ambient atmosphere at 110°C
114 overnight.

115 The Pd/AC-noCD sample was synthesized with a procedure identical to that used to
116 synthesize the Pd/AC(wash) hybrid, but in the absence of CD. Typically, 30 mg AA was
117 dissolved in 15 mL H₂O followed by the addition of the Na₂PdCl₄ solution. This mixture was
118 quickly added to the AC suspension and the reaction was continued for 3 hours.

119 The Pd/AC-1 sample was synthesized by using a procedure identical to that for preparing the
120 Pd/AC(wash) hybrid, with the exception that after adding the Na₂PdCl₄ solution to the aqueous
121 mixture containing 30 mg AA and 20 mg CD, the solution was stirred for 45 minutes to form a
122 Pd colloid. The resulting mixture was then added to the AC suspension followed by 3 hours of
123 stirring.

124 The Pd/AC-2 sample was synthesized with a procedure identical to that used to synthesize
125 the Pd/AC(wash) hybrid, but with an altered reaction sequence. Typically, the aqueous mixture
126 containing 30 mg AA and 20 mg CD was added to the AC suspension and the mixture was
127 stirred for 2 hours. The Na₂PdCl₄ solution was subsequently added to this suspension followed
128 by 3 hours of stirring.

129 2.3 Rinsing process

130 The Pd/AC(wash) sample was washed twice with acetone (50 mL each time) followed by
131 twice with water (50 mL each time). In a typical rinsing, the wet solid Pd/AC collected from the
132 previous filtration was dispersed in 50 mL acetone (or water) followed by 15 minutes of stirring
133 (1000 rpm). The suspension was then filtered with a Whatman filter paper.

134 The Pd/AC(no wash) sample was collected directly after the synthesis by filtration without
135 washing.

136 2.4 Characterization

137 The X-ray diffraction (XRD) patterns of the samples were recorded by using a D2-phaser
138 (Bruker) equipped with Cu radiation (30 kV, 10 mA) and a LYNXEYE detector that scanned 2θ
139 values between 10° and 90° . Transmission electron microscopy (TEM) images were obtained
140 with a Tecnai F30 microscope operated at 300 kV to analyze the morphologies of the Pd-based
141 catalysts. The catalysts were dispersed in acetone by using an ultrasonicator (SD-250H, Mujigae)
142 for 3 minutes and then dropped onto a carbon film containing holes supported by a 200 mesh
143 grid of copper. The system was then dried overnight. High-resolution X-ray photoelectron
144 spectroscopy (XPS) was performed on a Thermo VG Scientific Sigma Probe spectrometer with
145 an Al K α radiator, and the vacuum in the analysis chamber was maintained at 10^{-10} mbar.
146 Thermal gravimetric analysis (TGA) was carried out by using a Q 50 (TA Instruments, U.S.)
147 apparatus in air (flow rate 40 mLmin^{-1}). The samples were placed onto a platinum pan and
148 inserted into the furnace. The temperature was increased from room temperature to 850°C at a
149 rate of 20°Cmin^{-1} . The weight change was calculated based on the initial weight of the sample.
150 The elemental composition of C, N, and H in the samples were analyzed by combustion method
151 using an ELTRACS-800 analyzer (Germany). Ultraviolet-visible spectroscopy (UV-vis) was
152 carried out on a JASCO V-530 spectrophotometer (Japan) equipped with 10 mm quartz cells at
153 room temperature. The Pd loadings before and after 5 recycling runs were determined by using a
154 Thermo Scientific iCAP 6300 inductively coupled plasma optical emission spectroscopy (ICP-
155 OES) instrument.

156 2.5 Catalytic testing

157 2.5.1 Reduction of 4-nitrophenol

158 The reduction of 4-nitrophenol was carried out in a quartz cell at room temperature and was
159 *in situ* monitored by using UV-vis spectroscopy (JASCO V-530) scanning in the range 250–500
160 nm. In a typical reaction, 1 mL of an aqueous solution of 4-nitrophenol (0.1 mM) was added to 1
161 mL of an aqueous solution of NaBH₄ (10 mM), which results in a change in color from light
162 yellow to yellow green. After adding 0.1 mL of 0.05 mg.mL⁻¹Pd/AC(wash) catalyst to the
163 mixture, the cell was immediately placed into the UV-vis spectroscopy chamber for the
164 measurements. A similar procedure was applied to the samples Pd/AC-noCD and Pd/AC(no
165 wash).

166 2.5.2 Reduction of MB

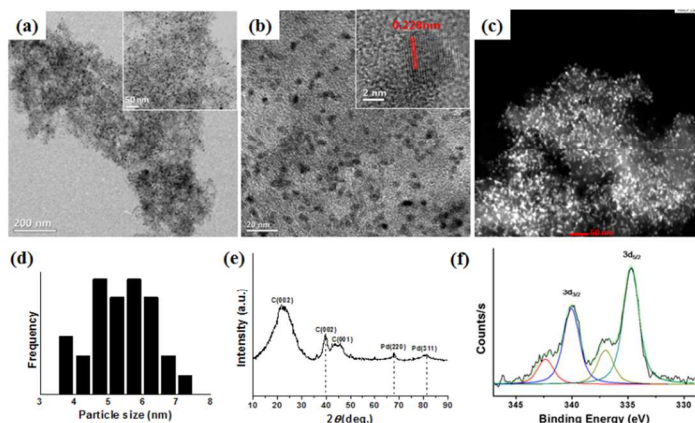
167 The reduction of MB was performed in a quartz cell at room temperature and was *in situ*
168 monitored with UV-vis spectroscopy (JASCO V-530) scanning in the range 550–725 nm.
169 Typically, 1 mL of an aqueous MB solution (10 mg.L⁻¹) was added to 1 mL of an aqueous
170 solution of NaBH₄ (10 mM). After adding 0.1 mL of 0.05 mg.mL⁻¹Pd/AC(wash) catalyst to the
171 mixture, the cell was rapidly placed into the UV-vis spectroscopy chamber for the measurements.
172 A similar procedure was applied to reduction processes with AC or without catalyst for
173 comparison.

174 2.5.3 Recyclable test of the Pd/AC(wash) catalyst

175 The stability of the Pd/AC(wash) catalyst was investigated by carrying out the same
176 reduction reactions with the magnification of 20 times. For each test, the reaction was performed
177 10 minutes. After that, the catalyst was recovered by a short centrifugation, washed with water
178 and EtOH before it was reused for the next catalytic cycle. The procedure was repeated totally 10
179 times.

180 3. Results and discussion

181 3.1 Characterization of the synthesized Pd/AC(wash) hybrid



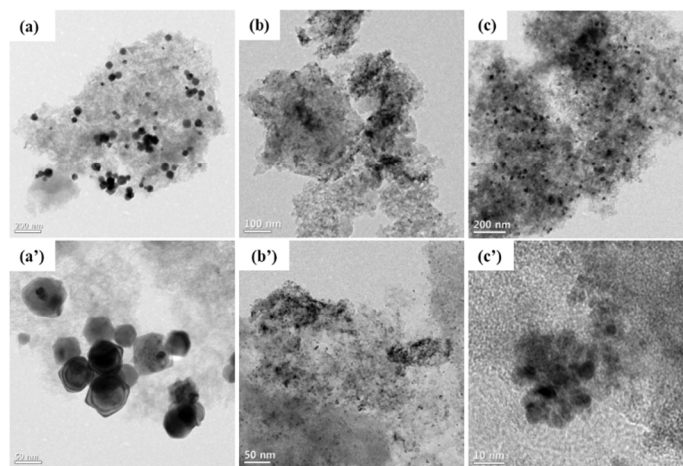
182

183 **Fig. 2** Characterization results for the Pd/AC(wash) hybrid. (a),(b) bright-field TEM images at various
184 magnifications,(c) dark-field TEM image, (d) Pd particle size distribution, (e) XRD pattern, and (e) XPS
185 data for the Pd 3d peaks.

186 The Pd/AC(wash) hybrid was synthesized by performing a facile one-step addition of an
187 aqueous solution containing a mixture of AA, CD, and Na₂PdCl₄ to an activated carbon (AC)
188 suspension, followed by the rinsing process (see Section 2.3). Transmission electron microscopy
189 (TEM) was carried out to examine the morphology of the synthesized Pd/AC(wash) hybrid. The
190 representative bright-field TEM images at various magnifications in Figs. 2(a) and (b) and the
191 typical dark-field TEM image in Fig. 2(c) show that the resulting Pd NPs are ultrafine and
192 homogeneously dispersed on the AC surface. The HR-TEM image in the inset of Fig. 2(b) of a
193 randomly selected Pd nanoparticle exhibits a lattice fringe distance of 0.228 nm, which
194 corresponds to the mean value of a typical (111) plane of an *fcc* Pd surface.²⁶ Moreover, the
195 TEM images reveal that the Pd particles mainly have sphere-like shapes. The particle size
196 histogram in Fig. 2(d) shows that the size distribution of the Pd NPs is uniform with sizes
197 predominantly in the range 4 to 7 nm. We also performed XRD analysis in the range 10°–90° to
198 examine the crystalline structure of the Pd/AC(wash) sample. The XRD pattern shown in Fig.
199 2(e) contains diffraction peaks at 2θ values of 40.1°, 68.2°, and 82°, which were assigned to the
200 (111), (220), and (311) planes of polycrystalline Pd NPs, respectively (JCPDS #46-1043). In
201 addition, broad peaks at 26° and 45° attributed to the typical (002) and (100) planes of the
202 hexagonal graphite structure of the AC support are also evident. The electronic state of the Pd
203 species in the synthesized Pd/AC(wash) hybrid was determined with the XPS technique. The Pd
204 3d XPS spectrum shown in Fig. 2(f) contains doublet peaks with binding energies at 334.7 eV

205 and 340.1 eV, which correspond to the species $\text{Pd}^0 3d_{5/2}$ and $\text{Pd}^0 3d_{3/2}$, respectively.²⁷ A small
206 portion of Pd^{2+} species ($3d_{5/2}$: 337 eV and $3d_{3/2}$: 342.3 eV) can be observed, which is probably
207 due to the fraction PdO or the interaction of Pd with oxygen from the carbon support. The XPS
208 data indicate that most of the Pd precursor has been reduced to metallic Pd^0 . The obtained results
209 clearly indicate the successful synthesis of a Pd/AC(wash) hybrid with highly dispersed and
210 ultrafine Pd NPs.

211 3.2 Effects of varying the reaction conditions



212

213 **Fig. 3** TEM images at various magnifications: (a), (a') Pd/AC-noCD sample, (b), (b') Pd/AC-1 sample,
214 and (c), (c') Pd/AC-2 sample.

215 To clarify the role of CD, we prepared a new sample by using a procedure identical to that
216 used to synthesize the Pd/AC(wash) hybrid, only without the presence of CD. Interestingly, after
217 adding the AA solution to the Na_2PdCl_4 solution, the mixture immediately turned black, which
218 indicates the formation of Pd NPs. The mixture was then rapidly added to the AC suspension
219 (denoted Pd/AC-noCD). The representative TEM images of the Pd/AC-noCD sample in Fig. 3(a)
220 and (a') reveal very large Pd particles with sizes larger than 50 nm, which suggests that CD is the
221 key factor to the synthesis of Pd/AC hybrids with ultrafine Pd NPs. We further investigated the
222 influence of the reaction conditions on the synthesis of the Pd/AC(wash) hybrid by preparing the
223 samples Pd/AC-1 and Pd/AC-2 with methods described in detail in the Experimental section.
224 Briefly, a mixture of CD, AA, and Na_2PdCl_4 was allowed to react for 45 minutes to form
225 colloidal Pd NPs, and was subsequently added to the AC suspension to prepare the Pd/AC-1

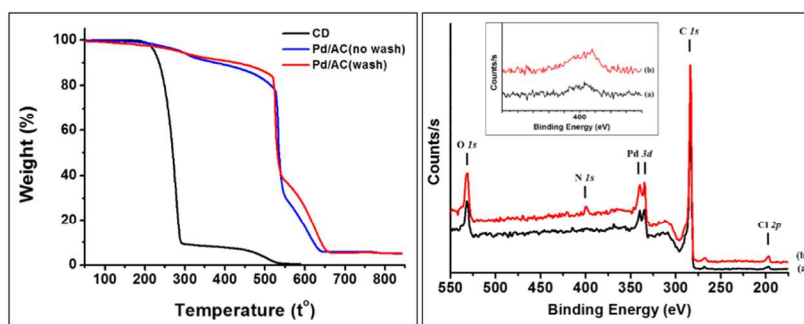
226 sample. The Pd/AC-2 sample was prepared by adding the Na_2PdCl_4 solution to a mixture
227 containing AC, AA, and CD. Typical TEM images of the Pd/AC-1 sample are shown in Fig. 3(b)
228 and (b'), and reveal that the Pd NPs are not homogeneously deposited on the AC support, which
229 is most likely due to the agglomeration of Pd NPs when they are formed in the colloid (Fig. S1).
230 The TEM images of the Pd/AC-2 sample in Fig. 3(c) and (c') display large Pd particles with
231 sizes above 20 nm and irregular shapes. These TEM data demonstrate that a precise preparation
232 is critical to achieving Pd/AC hybrids with ultrafine and well-dispersed Pd NPs.

233 Based on the data obtained from the influence of various synthetic conditions, we can
234 propose the formation of Pd NPs as follow. In the sample Pd/AC(wash), the mixture of AA, CD,
235 and Na_2PdCl_4 was rapidly added to the AC suspension; hence, Pd NPs growing in this sample
236 have a similar strategy like that growing in the Pd colloid (Fig. S1). Pd nuclei are formed in the
237 solution and they grow to form Pd NPs while CD molecules play role as capping agents. In the
238 presence of AC, these Pd nuclei anchor on the AC surface and gradually grow to form Pd NPs.
239 Because the Pd nuclei are homogeneously formed in the solution, the growth of Pd NPs on AC
240 surface is well-dispersed with uniform size. On the other hand, the Pd/AC-2 sample was
241 prepared by adding Na_2PdCl_4 to the mixture of AA, CD, and AC. In this case, the AC surface is
242 already well-covered by layers of CD molecules; therefore, the Pd nuclei formed on the sample
243 Pd/AC-2 actually anchor on the CD-covered AC surface. When these nuclei grow larger, they
244 have a tendency to aggregate to reduce the surface energy. Since the adsorption of CD on AC
245 surface is sufficiently weak,²⁸ these Pd nuclei can migrate and aggregate during their growth;
246 consequently, form Pd particles with irregular shape and big size.

247 **3.3 Removal of the CD capping agent**

248 Although capping agents ensure the homogeneous dispersion of NPs on supports, their
249 presence restricts the free access of reactants to active sites on the particle surfaces, which leads
250 to reduced catalytic activity. Thus, the depletion of the capping agent to attain an ultrapure
251 surface of particles after the synthesis has generally been a crucial part of the process for
252 preparing catalysts with the desired performance. Most capping agents reported in the literature
253 are high molecular weight organic compounds that bind strongly to the surface of particles,
254 resulting in severe purification difficulties.²⁹ In the present approach, the capping agent CD and

255 byproducts of the synthesis were found to be easily removed with a simple rinsing process.
 256 Briefly, the synthesized Pd/AC hybrid was washed twice with acetone followed by twice with
 257 water; this sample is denoted Pd/AC(wash) to distinguish it from the Pd/AC sample collected
 258 without washing, Pd/AC(no wash). TEM study of these samples shows similar to each other (Fig.
 259 S2), suggesting that the distribution and morphology of Pd NPs are not affected by the washing
 260 process. The complete removal of CD was demonstrated by performing TGA, EDS, elementary
 261 analysis, and XPS methods.



262
 263 **Fig. 4** Left panel: TGA data for CD (black), and for the Pd/AC hybrids before washing (blue) and after
 264 washing (red). Right panel: XPS spectra for (a) Pd/AC(wash) and (b) Pd/AC(no wash). The inset shows
 265 high-resolution scans of the N 1s region.

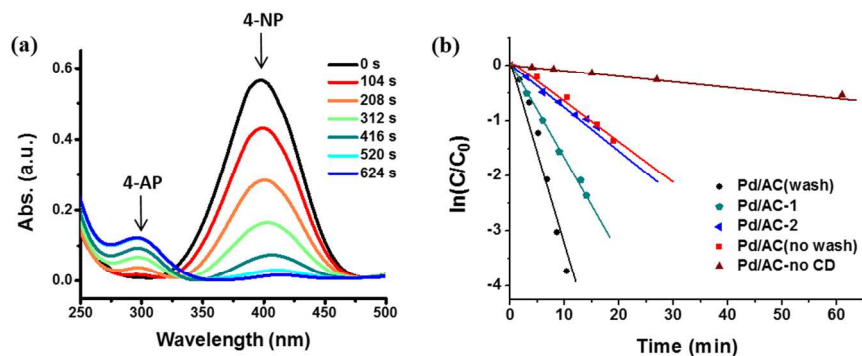
266 TGA was conducted for the two samples in the range 50°C to 850°C to study their thermal
 267 behaviors and to compare their weight losses. TGA was also carried out for CD as a reference.
 268 As shown in the panel on the left of Fig. 4, approximately 90% of the mass of CD decomposes in
 269 the range 200–300°C, and it completely decays above 550°C. The Pd/AC(wash) and Pd/AC(no
 270 wash) samples exhibit similar thermal behaviors. An initial weight loss of 5% at 300°C followed
 271 by a ~15% mass loss at 550°C were observed, which are due to the removal of oxygen-functional
 272 groups present on AC and residual CD. Subsequently, the TGA curves of these samples rapidly
 273 drop to 5% wt in the range 550–650°C, which is assigned to the decomposition of their graphitic
 274 carbon components.³⁰ Above 650°C, the two samples retain only a mass of approximately 5% wt.
 275 It is worth to point out that the Pd/AC(no wash) sample undergoes slightly more weight loss in
 276 the range 350–550°C than the Pd/AC(wash) sample. Since the two samples are identical with
 277 only the exception of the washing step, this minor difference in weight loss must be due to
 278 remaining CD. The results obtained with TGA indicate that the washing step effectively removes
 279 the residual CD; however, this weight loss comparison can only relatively evaluate the removal

280 of CD and it does not directly assess the depletion of CD. We further analyzed the elimination of
281 CD quantitatively by tracking the presence of nitrogen in each sample, since a CD molecule
282 contains two N atoms. EDS, elementary analysis, and XPS, which are very sensitive and helpful
283 techniques generally used to detect the presence of capping agents after their removal,³¹⁻³³ were
284 carried out to determine the amounts of N in the two samples.

285 The quantity of N in the sample Pd/AC(wash) was determined by recording an EDS
286 spectrum of the area marked as a small red spot in the corresponding dark-field image (Fig.S3).
287 The peaks near 0.28 and 2.90 keV are due to the K-shell emission of C and the L-shell emission
288 of Pd, respectively.³⁴ There is no peak at 0.38 keV corresponding to the K-shell emission of N,
289 which indicates that almost all of the capping agent CD has been removed. Moreover, the data
290 obtained from the elementary analysis (Table S1) reveals that the Pd/AC(wash) sample contains
291 a very small amount of N element (0.45%) compared to that in the Pd/AC (no wash) sample
292 (2.48%). The panel on the right of Fig. 4 shows the XPS survey spectra of the Pd/AC hybrid
293 before and after the rinsing process. Both the Pd/AC(wash) and the Pd/AC(no wash) samples
294 contain only the elements O, N, Pd, C, and Cl, which is in agreement with the chemical
295 compositions of the starting materials used in the synthesis. Note that the N 1s and Cl 2p peaks
296 are clearly detected in the spectrum of the sample Pd/AC(no wash), but are not present in the
297 spectrum of the sample Pd/AC(wash), indicating the effective removal of CD and byproducts by
298 the washing process. The high-resolution scans of the N 1s region for the sample Pd/AC(wash)
299 in the inset of the panel on the right of Fig. 4 contain a very low intensity peak, which confirms
300 that the residual CD is almost completely depleted by the rinse. It has been reported that CD
301 interacts weakly with the Pd surface through the π -bonding system (the quinoline moiety nearly
302 parallel to the Pd surface) or through the σ -bonding system (the N lone pair predominates and
303 induces a tilting of the ring with respect to Pd).²⁸ Thus, the straightforward removal of CD by
304 washing is most likely due to these weak interactions. The results obtained from the EDS,
305 elemental analysis, and XPS demonstrate that a simple washing process can almost completely
306 eliminate residual CD.

307 **3.4 Catalytic performance**

308 *Reduction of 4-nitrophenol*



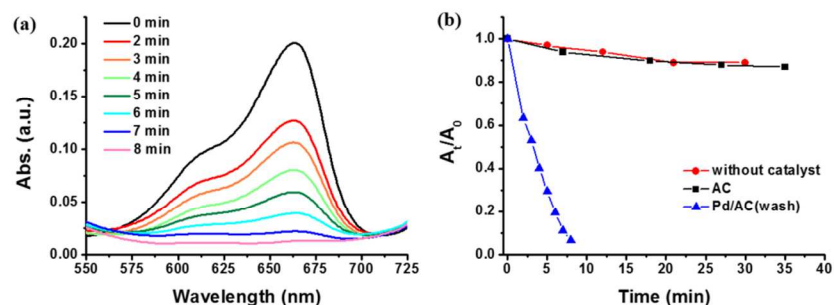
309
 310 **Fig. 5** (a) UV-vis spectra of the reduction of 4-nitrophenol in aqueous solution using the catalyst
 311 Pd/AC(wash), (b) the relationships between $\ln(C/C_0)$ and reaction time for the synthesized catalysts.

312 Like other aromatic nitro-compounds, 4-nitrophenol is a hazardous and carcinogenic
 313 chemical used as a main component of pesticides, plasticizers, and herbicides,³⁵ whereas 4-
 314 aminophenolis an important intermediate for industrial manufacturing processes, including the
 315 production of analgesic drugs and anticorrosion lubricants.³⁶ The development of efficient
 316 approaches for the reduction of nitro to amino groups based on novel catalysts has attracted great
 317 attention in synthetic organic chemistry.³⁷ In the field of catalysis, the borohydride reduction of
 318 4-nitrophenol to 4-aminophenol has generally been used as a benchmark system for the
 319 assessment of the catalytic abilities of metal-based materials.^{38,39} In the present study, this
 320 reaction was carried out in an aqueous medium at room temperature to evaluate the catalytic
 321 activity of the prepared Pd/AC(wash) hybrid; the kinetics of the reaction were monitored with
 322 UV-vis spectroscopy in the range 250–500 nm.

323 The UV-vis spectra of the reduction of 4-nitrophenol in aqueous solution using the catalyst
 324 Pd/AC(wash) are shown in Fig. 5(a). As the reaction time increases, the intensity of the
 325 absorption peak at 400 nm, which is due to 4-nitrophenolate ions in alkaline conditions,
 326 decreases gradually and a new absorption peak appears at 300 nm, which is due to 4-
 327 aminophenol. The peak at 400 nm disappeared after 9 minutes, which indicates complete
 328 conversion. It is worth to note that there is no induction time for this reaction as it proceeded
 329 immediately after the addition of the Pd/AC(wash) catalyst, unlike the results from other
 330 reported studies.^{40,41} This advantage is due to the depletion of the CD capping agent, which
 331 enables the easy and rapid access of reactants to the purified Pd surfaces. Control experiments

332 were also carried out with the Pd/AC-noCD, Pd/AC(no wash), Pd/AC-1, and Pd/AC-2 samples
333 as catalysts (Fig. S4). In all experiments, similar adsorption behaviors are observed in the UV-vis
334 spectra, but the reactions required much more time. Since we utilized a concentration of NaBH_4
335 in significant excess with respect to the concentration of 4-nitrophenol, the reaction is considered
336 to follow pseudo-first-order kinetics with respect to 4-nitrophenol (or rather, the 4-nitrophenolate
337 ion). Fig. 5(b) shows the relatively linear dependence of $\ln(C/C_0)$ on the reaction time, as
338 expected for a first-order reaction. The kinetic rate constant k of the reaction when we used the
339 catalyst Pd/AC(wash) was calculated to be 0.32 min^{-1} , which is significantly higher than that
340 obtained with the catalysts Pd/AC(no wash) (0.07 min^{-1}), Pd/AC-noCD (0.01 min^{-1}), Pd/AC-1
341 (0.17 min^{-1}), and Pd/AC-2 (0.08 min^{-1}). These results demonstrate that the very high reactivity
342 of the Pd/AC(wash) catalyst is solely due to the ultrafine, well-dispersed, and purified Pd NPs
343 present on the AC support, and further confirm the efficient removal of CD by the washing
344 process. Moreover, this rate constant is also comparable with the excellent k values obtained in
345 other corresponding studies.⁴²⁻⁴⁴

346 *Reduction of methylene blue (MB)*



347
348 **Fig. 6** (a) Absorption spectra of a MB solution in the presence of the catalyst Pd/AC(wash), (b) Plots of
349 A_t/A_0 vs time for the borohydride reductions of MB solutions.

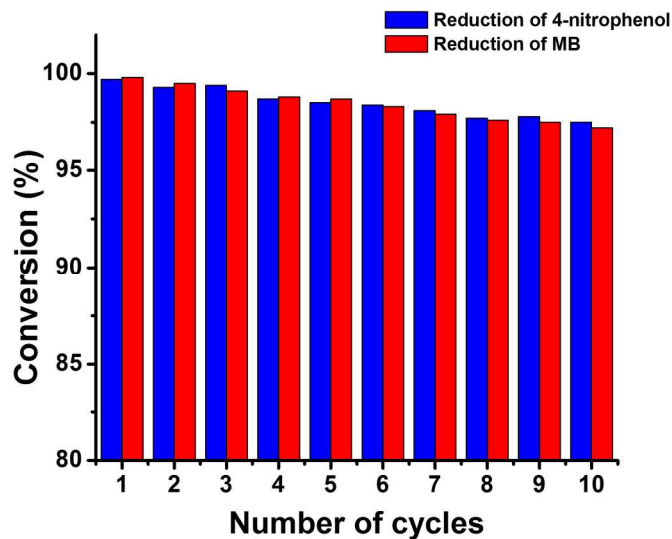
350 The excellent catalytic ability of the synthesized Pd/AC(wash) catalyst in the reduction of 4-
351 nitrophenol inspired us to continue testing its catalytic activity in the degradation of MB dye,
352 which is a toxic contaminant⁴⁵ released to wastewater during the industrial manufacture of
353 textiles, paper, and paint. MB solutions are dark blue, and exhibit a strong absorption peak in

354 visible light (550–750 nm) whereas the reduced MB solution is colorless, so UV-vis
355 spectroscopy is commonly used to monitor this reduction process.

356 Fig. 6(a) shows the UV-vis spectra obtained during the MB degradation by NaBH₄ in the
357 presence of the Pd/AC(wash) catalyst. The intensity of the absorption peak at 664 nm, which is
358 assigned to the dark blue MB solution, continuously decreases as the degradation proceeds, and
359 has completely disappeared within 8 minutes. Keeping in mind that AC is generally used as a
360 good absorbent for dyes because of its amorphous structure and high surface area,⁴⁶ we also
361 carried out the reduction of MB in the presence of AC alone (Fig. S5(a)) to elucidate the
362 efficiency of the Pd/AC(wash) catalyst. The plot in Fig. 6(b) provides the relationship between
363 the ratio A_t/A_0 (the ratio of the intensity of the absorption peak at 664 nm at reaction time t and
364 the initial intensity) and the reaction time. As expected, the presence of AC decolorizes the MB
365 solution but only to a small degree and the reaction proceeds very slowly, which indicates that
366 only a small amount of MB is absorbed by AC; hence, the absorption capacity of AC is
367 negligible in the presence of the Pd/AC(wash) catalyst. In addition, almost no change in the color
368 of the MB solution was observed when we performed the reaction without catalyst (Fig. S5(b)),
369 indicating that the Pd NPs are the active sites for the reduction of MB. The UV-vis data obtained
370 from the MB reduction further confirm the high catalytic ability of the Pd/AC(wash) hybrid.

371 **3.5 Catalyst recycling**

372 The recyclability of catalysts is an important criterion to evaluate the practical applications
373 of heterogeneous catalysts. As shown in Fig. 7, the Pd/AC(wash) catalyst exhibits highly stable
374 and reusable properties. Although a slight decrease in conversion is observed in both reduction
375 reactions, their conversions can achieve above 98.5% after 5 consecutive runs with only a small
376 fraction of Pd leaching, as determined by the ICP analyses (Table S2). A further investigation of
377 catalytic stability to 10 consecutive cycles shows that both reactions still have very high
378 conversions which are over 97% (Fig. 7). The high stability of this catalyst makes it more
379 economical and applicable for catalytic industry.



380
381 **Fig. 7** The reusability of the Pd/AC(wash) catalyst for the reduction of 4-nitrophenol (blue) and MB (red).

382 4. Conclusion

383 A facile one-pot green synthesis of Pd/AC hybrids with uniform and well-dispersed Pd NPs
384 was successfully achieved by using CD, a naturally available and environmentally friendly
385 compound, as a capping agent for the first time. CD was found to be easily eliminated after the
386 synthesis, which is a significant advantage over traditional capping agents. The synthesized
387 hybrid was found to exhibit very high catalytic activities because of its ultrafine, homogeneously
388 dispersed and purified Pd NPs. The application of this facile and green route for the synthesis of
389 high-performance nanocatalysts using other catalytically active metals (Pt, Ag, *etc.*) supported on
390 different carbon materials, such as graphene and carbon nanotubes, is ongoing. The present study
391 furthers the quest for novel, naturally benign sources for the synthesis of heterogeneous catalysts,
392 and the employment of CD can be extended to the green syntheses of other metal-based hybrids.

393 Acknowledgements

394 This research was supported by the National Research Foundation of Korea (NRF) funded
395 by the Korea government (MSIP) (No. 2014004111 and No. 20090083525).

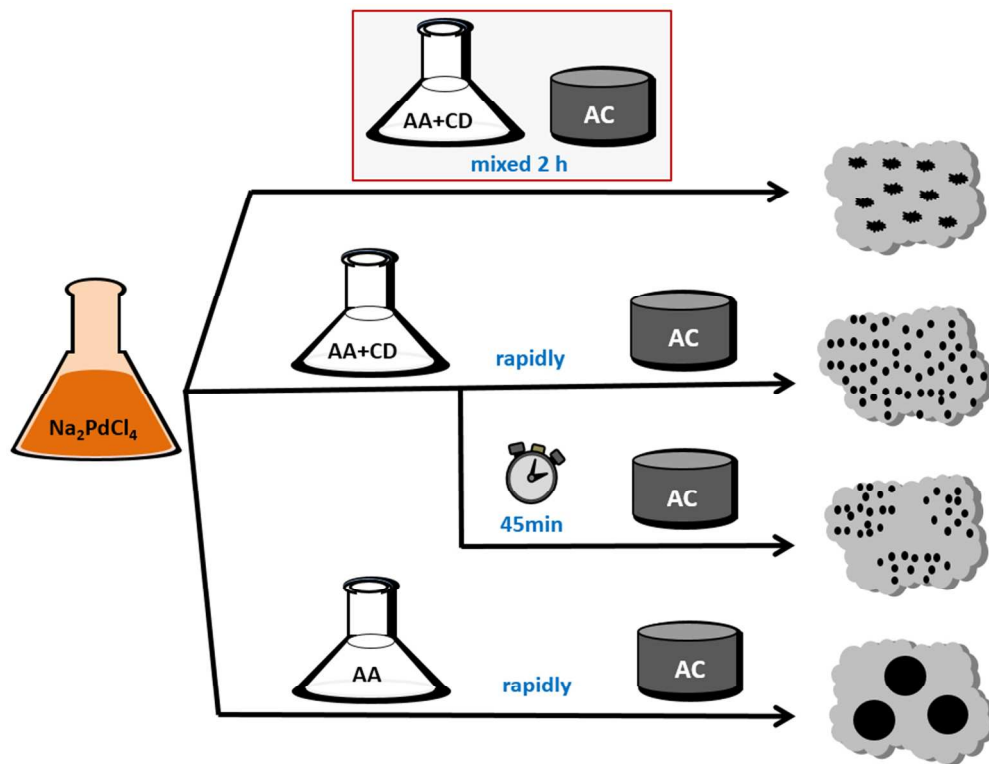
396

397 **References**

- 398 1 Á. Molnár, *Chem. Rev.*, 2011, **111**, 2251-2320.
- 399 2 R. Chinchilla and C. Nájera, *Chem. Rev.*, 2013, **114**, 1783-1826.
- 400 3 J. Le Bras and J. Muzart, *Chem. Soc. Rev.*, 2014, **43**, 3003-3040.
- 401 4 T. S. Bui Trung, Y. W. Kim, S. H. Kang, H. G. Lee and S. H. Kim, *Catal. Commun.*,
- 402 2015, **66**, 21-24.
- 403 5 T. Sun, Z. Zhang, Ju. Ziao, C. Chen, F. Xiao, S. Wang and Y. Liu, *Sci. Rep.*, 2013, **3**,
- 404 2527.
- 405 6 K. Yan, T. Lafleur, G. Wu, J. Liao, C. Ceng and X. Xie, *Appl. Catal. A*, 2013, **468**, 52-58.
- 406 7 S. Moussa, A. R. Siamaki, B. F. Gupton and M. S. El-Shall, *ACS Catal.*, 2012, **2**, 145-
- 407 154.
- 408 8 T. S. Bui Trung, Y. W. Kim, S. H. Kang, S. H. Kim and H. G. Lee, *Appl. Catal. A*, 2015,
- 409 [doi:10.1016/j.apcata.2015.08.011](https://doi.org/10.1016/j.apcata.2015.08.011)
- 410 9 Z. Zhang, Y. Dong, L. Wang and S. Wang, *Chem. Commun.*, 2015, **51**, 8357-8360.
- 411 10 Z. Wang, J. Yan, H. Wang, Y. Ping and Q. Jiang, *Sci. Rep.*, 2012, **2**, 598.
- 412 11 F. Rodríguez-reinoso, *Carbon*, 1998, **36**, 159-175.
- 413 12 J. A. Dahl, B. L. S. Maddux and J. E. Hutchison, *Chem. Rev.*, 2007, **107**, 2228-2269.
- 414 13 M. N. Nadagouda and R. S. Varma, *Green Chemistry*, 2006, **8**, 516-518.
- 415 14 M. N. Nadagouda and R. S. Varma, *Green Chemistry*, 2008, **10**, 859-862.
- 416 15 N. N. Mallikarjuna and R. S. Varma, *Cryst. Growth Des.*, 2007, **7**, 686-690.
- 417 16 J. M. Patete, X. Peng, C. Koenigsmann, Y. Xu, B. Karn and S. S. Wong, *Green*
- 418 *Chemistry*, 2011, **13**, 482-519.
- 419 17 P. J. Straney, L. E. Marbella, C. M. Andolina, N. T. Nuhfer and J. E. Millstone, *J. Am.*
- 420 *Chem. Soc.*, 2014, **136**, 7873-7876.
- 421 18 W. Yang, Y. Wang, J. Li and X. Yang, *Ener. Envi. Sci.*, 2010, **3**, 144-149.
- 422 19 *Cinchona Alkaloids in Synthesis and Catalysis: Ligands, Immobilization and*
- 423 *Organocatalysis*, ed. C.E. Song, Wiley-VCH, 2009.
- 424 20 T. Marcelli, *WIREs: Comput. Mol. Sci.*, 2011, **1**, 142-152.
- 425 21 T. Mallat, E. Orglmeister and A. Baiker, *Chem. Rev.*, 2007, **107**, 4863-4890.
- 426 22 G. D. H. Dijkstra, R. M. Kellogg and H. Wynberg, *J. Org. Chem.*, 1990, **55**, 6121-6131.

- 427 23 G. D. H. Dijkstra, R. M. Kellogg, H. Wynberg, J. S. Svendsen, I. Marko and K. B.
428 Sharpless, *J. Am. Chem. Soc.*, 1989, **111**, 8069-8076.
- 429 24 H. Bönemann and G. A. Braun, *Angew. Chem. Int. Ed.*, 1996, **35**, 1992-1995.
- 430 25 F. Kirby, C. Moreno-Marrodan, Z. Baan, B. F. Bleeker, P. Barbaro, P. H. Berben and P.
431 T. Witte, *ChemCatChem*, 2014, **6**, 2904-2909.
- 432 26 G. J. Thomas, R. W. Siegel and J. A. Eastman, *Mat. Res. Soc. Symp. Proc.*, 1989, **153**,
433 13-20.
- 434 27 K. Yan, T. Lafleur and J. Liao, *J. Nanopart. Res.*, 2013, **15**, 1906.
- 435 28 D. Ferri, *J. Catal.*, 2002, **210**, 160-170.
- 436 29 Z. Q. Niu and Y. D. Li, *Chem. Mater.*, 2014, **26**, 72-83.
- 437 30 R. Yang, T. R. Dahn and J. R. Dahn, *J. Electrochem. Soc.*, 2009, **156**, B493-B498.
- 438 31 N. Naresh, F. G. S. Wasim, B. P. Ladewig and M. Neergat, *J. Mater. Chem. A*, 2013, **1**,
439 8553-8559.
- 440 32 M. Crespo-Quesada, J. M. Andanson, A. Yarulin, B. Lim, Y. Xia and L. Kiwi-Minsker,
441 *Langmuir*, 2011, **27**, 7909-7916.
- 442 33 S. K. Kim, C. H. Kim, J. H. Lee, J. Y. Kim, H. J. Lee and S. H. Moon, *J. Catal.*, 2013,
443 **306**, 146-154.
- 444 34 A. C. Thompson, *X-ray Data Booklet*, Lawrence Berkeley National Laboratory,
445 University of California, 3rd ed., Sep. 2009.
- 446 35 P. Kovacic and R. Somanathan, *J. Appl. Toxicol.*, 2014, **34**, 810-824.
- 447 36 S. Mitchell, *Kirk-Othmer Encyclopedia of Chemical Technology*, Wiley-Interscience,
448 New York, 4th ed., 1992, vol. II, p. 580.
- 449 37 H. U. Blaser, H. Steiner and M. Studer, *ChemCatChem*, 2009, **1**, 210-221.
- 450 38 H. Li, S. Gan, D. Han, W. Ma, B. Cai, W. Zhang, Q. Zhang and L. Niu, *J. Mater. Chem.*
451 *A*, 2014, **2**, 3461-3467.
- 452 39 S. K. Das, C. Dickinson, F. Lafir, D. F. Brougham and E. Marsili, *Green Chemistry*,
453 2012, **14**, 1322-1334.
- 454 40 S. Wunder, F. Polzer, Y. Lu, Y. Mei and M. Ballauff, *J. Phys. Chem. C*, 2010, **114**,
455 8814-8820.

- 456 41 Y. Gao, X. Ding, Z. Zheng, X. Cheng and Y. Peng, *Chem. Commun.*, 2007, **36**, 3720-
457 3722.
- 458 42 Y. Fang and E. Wang, *Nanoscale*, 2013, **5**, 1843-1848.
- 459 43 X. Wu, C. Lu, W. Zhang, G. Yuan, R. Xiong and X. Zhang, *J. Mater. Chem. A*, 2013, **1**,
460 8645-8652.
- 461 44 H. Li, L. Han, J. Cooper-White and I. Kim, *Green Chemistry*, 2012, **14**, 586-591.
- 462 45 P. R. Ginimuge and S. D. Jyothi, *J. Anaesthesiol. Clin. Pharmacol.*, 2010, **26**, 517-520.
- 463 46 A. Demirbas, *J. Hazard. Mater.*, 2009, **167**, 1-9.



211x164mm (120 x 120 DPI)